Dynamical lattice gases and inherent structure in condensed phases

F. H. Stillinger
AT&T Bell Laboratories, Murray Hill, New Jersey 07974

(Received 17 July 1987; accepted 15 September 1987)

The nature of structural order and basic kinetic processes in condensed phases theoretically can be clarified by quenching to mechanically stable particle packings, the relevant "inherent structure". Numerically locating these potential energy minima in realistic models for various substances is often a very demanding task. A class of many-body systems, "dynamical lattice gases," is introduced for which the steepest-descent quenching is particularly simple. The resulting packings place particles on sites of a regular array, the distribution of energies of those packings can be obtained from the solution of a related Ising model, and transition states between interconvertible packings are trivial to locate. Some elementary analytical results have been obtained for vibrational free energies of the packings. Some versions of these models, notably the quarter-filled face-centered-cubic case, are well suited for study of liquid-phase supercooling and formation of low-temperature amorphous solids.

I. INTRODUCTION

The canonical partition function $Z_N(\beta)$ provides a connection between equilibrium thermodynamic properties at inverse temperature $\beta = (k_B T)^{-1}$ and the atomic-scale interactions that operate between the N particles involved. Assuming that those particles are structureless and can be adequately described by classical statistical mechanics, $Z_N(\beta)$ adopts the following standard form[1]:

$$Z_N(\beta) = (\lambda_T^{DN} N!)^{-1} \int d\mathbf{r}_1 \cdots \int d\mathbf{r}_N \exp(-\beta\Phi) . \tag{1.1}$$

Here λ_T represents the mean thermal deBroglie wavelength for the particles (all assumed to be identical), D is the space dimension, and Φ denotes the potential energy of interaction which depends only on the particle positions $\mathbf{r}_1 \cdots \mathbf{r}_N$.

Except for low density or high temperature limiting cases, no general techniques are available to evaluate the multidimensional configuration integral in Eq. (1.1). Nevertheless the mathematical character of $Z_N(\beta)$ can be illuminated by a series of transformations which reduces it formally to a simple quadrature.[2–5] This procedure will now be reviewed briefly to provide a clarifying basis for the remainder of the paper.

The potential energy Φ is bounded below, symmetric under particle interchange, and differentiable, when all of $\mathbf{r}_1 \cdots \mathbf{r}_N$ are distinct. The shape of the Φ hypersurface over the DN-dimensional configuration space leads to a natural and exhaustive division of that space into "basins" B_α, each one of which surrounds a single relative minimum α of the potential energy function Φ. The set of configurations $\mathbf{r}_1 \cdots \mathbf{r}_N$ which compose B_α are just those starting points for a steepest-descent path on the Φ hypersurface which converge onto relative minimum α.

Particle interchange symmetry implies that each basin B_α is but one among $N!$ equivalent basins that differ only by particle coordinate permutations. Taking this feature into account, Eq. (1.1) may be rewritten,

$$\begin{aligned} Z_N(\beta) &= \lambda_T^{-DN} \sum_\alpha{}' \int_{B_\alpha} \exp[-\beta\Phi(\mathbf{r})]\,d\mathbf{r} \\ &= \lambda_T^{-DN} \sum_\alpha{}' \exp(-\beta\Phi_\alpha) \\ &\quad \times \int_{B_\alpha} \exp[-\beta\Delta_\alpha\Phi(\mathbf{r})]\,d\mathbf{r} . \end{aligned} \tag{1.2}$$

Here the primed α sum covers only inequivalent basins, and the DN-component vector $\mathbf{r}$ comprises all particle positions. The latter form in Eq. (1.2) separates Φ into its value at minimum α, namely Φ_α, plus its positive deviation $\Delta_\alpha\Phi$ elsewhere within B_α.

It is useful next to classify the relative minima by ϕ, their depth on a per particle basis:

$$\phi = \Phi_\alpha / N . \tag{1.3}$$

In view of the fact that in the large-N limit the number of inequivalent minima is expected to rise exponentially with N, it is natural to introduce a distribution function for minima with the form

$$G_N(\phi) \cong \exp[N\sigma(\phi)] , \tag{1.4}$$

where σ is N = independent.

A vibrational free energy per particle $f_v(\beta,\phi)$ can be defined for those basins whose depths are arbitrarily close to ϕ (denoted by a doubly primed sum):

$$\exp[-\beta N f_v(\beta,\phi)] \cong \left\{ \sum_\alpha{}'' \int_{B_\alpha} \exp[-\beta\Delta_\alpha\Phi]\,d\mathbf{r} \right\} \Big/ \sum_\alpha{}'' 1 . \tag{1.5}$$

As the notation indicates f_v is expected to be independent of N in the large-N limit, but to retain a dependence on the depth of the group of basins considered.

Employing definitions (1.3)–(1.5), it is straightforward to convert the α sum in Eq. (1.2) to a ϕ integral:

$$Z_N(\beta) \cong \lambda_T^{-DN} \int \exp\{N[\sigma(\phi) - \beta\phi - \beta f_v(\beta,\phi)]\}\,d\phi . \tag{1.6}$$

For any realistic interaction potential, the distribution of

 0021-9606/88/010380-06$02.10

basin depths, and therefore the ϕ integral in Eq. (1.6), will have finite upper and lower limits.

Because N is large, the maximum of the integrand in Eq. (1.6) provides the leading-order contribution to this integral. Specifically,

$$\ln[\lambda_T^{DN} Z_N] \sim N\{\sigma[\phi_m(\beta)] - \beta\phi_m(\beta) - \beta f_v[\beta,\phi_m(\beta)]\}, \quad (1.7)$$

where ϕ_m maximizes the right-hand side for any given β. The quantity $\phi_m(\beta)$ identifies the depth of that population of basins within which the system is virtually certain to be found at the prevailing temperature. If the system were to undergo a first-order melting transition, ϕ_m would jump from a low value corresponding to crystalline arrangements of particles to a higher value corresponding to amorphous packings.

Several theoretical benefits flow from this representation of the many-body problem. One of these is the demonstration (for simple atomic substances at least) that a virtually temperature-independent inherent structure underlies the liquid phase, which is revealed by steepest-descent mapping onto minima of Φ.[6–8] Another is the extension of the Lindemann melting criterion for crystals to an analogous criterion for the freezing of liquids.[9] A third benefit is that specific groups of atomic motions with bistable character can be identified in models for low-temperature amorphous deposits, thus providing contact with those properties of real amorphous materials which appear to be affected at low temperature by two-level systems.[4,10] Finally, this approach seems to be useful in understanding basic molecular processes that control the behavior of dense chemically reactive liquids.[11–14]

Unfortunately, information remains scanty regarding basin geometries and the fundamental quantities σ, f_v, and ϕ_m in Eq. (1.7). Thermodynamic, mechanical, and spectroscopic measurements on real substances offer some guidance, and a variety of computer simulation studies provides an independent source of partial insight.[15,16] What has thus far been largely missing are analytically tractable models for which σ, f_v, and ϕ_m could be evaluated. The objective of this paper is to propose a class of such models, to demonstrate their properties in light of the preceding discussion, and to point out conceptual implications for real materials.

Section II provides a general definition of the "dynamical lattice gas models," stressing that their potential energy minima can trivially be put into one-to-one correspondence with the discrete states of an associated Ising model. Section III restricts attention to a specific square planar model, and exhibits the exact $\sigma(\phi)$ for the half-monolayer density in terms of the closed-form solution for the two-dimensional square Ising model at zero field (first derived by Onsager[17]). The role of vibrational motions in this latter specific case is analyzed in Sec. IV. Section V contains some concluding remarks concerning dynamical simulation, and extensions of the models to study glass transitions and low-temperature amorphous states in multicomponent systems and in systems with structured particles.

II. ADSORPTION MODELS

We will be concerned from the outset with the case of N structureless particles that move in D-dimensional space, with Hamiltonian (H) consisting of the usual kinetic (K) and potential (Φ) terms:

$$H = K + \Phi . \quad (2.1)$$

The potential energy has a single-particle part (Φ_0) and a particle interaction part (Φ_1). Including a variable coupling constant (λ) for the latter, we write

$$\Phi = \Phi_0 + \lambda\Phi_1 , \quad (2.2)$$

wherein

$$\Phi_0(\mathbf{r}_1 \cdots \mathbf{r}_N) = \sum_{i=1}^{N} U(\mathbf{r}_i) . \quad (2.3)$$

The single-particle potential U is intended to represent adsorption on (or absorption within) a periodic static substrate (or host) material. Consequently $U(\mathbf{r})$ will itself be periodic, and we shall assume it is bounded, continuous, and at least twice differentiable. Within the finite D-dimensional volume available to the N particles, $U(\mathbf{r})$ will present some number M of replicas of a fundamental unit cell.

For simplicity it will be presumed that $U(\mathbf{r})$ possess only a single minimum within its unit cell, the "adsorption site," whose depth will be denoted $-U_0$. At low kinetic energies an isolated particle would execute nearly harmonic oscillations about that site, while at higher kinetic energies the motions would be anharmonic or even unbound to that site. If the coupling constant λ were set to zero so that $\Phi = \Phi_0$, all minima of Φ would have the same depth $-NU_0$, and would correspond to each of the N particles located exactly at an adsorption site. The number of such Φ minima is trivial to calculate:

$$\Omega_0 = M^N . \quad (2.4)$$

In the limit of large M and N this can be put into the asymptotically correct alternative form:

$$\Omega \cong N! \exp(\nu_0 N) , \quad \nu_0 = 1 + \ln(M/N) . \quad (2.5)$$

The role of interparticle potential Φ_1 is (a) to prevent multiple occupancy of sites by two or more particles (requiring $N \leqslant M$), and (b) to provide finite interactions between pairs of particles located within nearest-neighbor unit cells. The first of these requirements eliminates many of the particle configurations which were counted in Eq. (2.4) as Φ_0 minima. In fact it is possible (see below) to choose Φ_1 so that all configurations which are single-occupancy Φ_0 minima continue to be relative minima with Φ_1 present. That is, all configurations with single particles exactly at adsorption sites will still be mechanically stable, but Φ_1 will have broken the $\lambda = 0$ depth degeneracy. Under this circumstance the diminished number of Φ minima is now

$$\Omega = M!/(M-N)! \cong N! \exp(\nu N) , \quad (2.6)$$
$$\nu = \left(\frac{M}{N}\right)\ln\left(\frac{M}{N}\right) - \left(\frac{M-N}{N}\right)\ln\left(\frac{M-N}{N}\right) .$$

This agrees with the ν_0 expression (2.5) only through linear order in N/M.

The interparticle interactions contained in Φ_1 will involve only additive pair terms, and these will vanish identically for all pairs of particles in cells more widely separated than nearest neighbors:

$$\Phi_1(\mathbf{r}_1 \cdots \mathbf{r}_N) = \sum_{\langle i,j \rangle} V(\mathbf{r}_i,\mathbf{r}_j) \,. \tag{2.7}$$

Here the $\langle i,j \rangle$ sum comprises all nearest-neighbor pairs. In order to guarantee that the single occupancy restriction be satisfied it suffices to let V become very large and positive for two particles in the same cell. Dynamically this means that if a particle has a trajectory intersecting the boundary of an already occupied cell, it must undergo specular reflection at that boundary. Within the portion of the full DN-dimensional configuration space which displays only single occupancy, we will demand that Φ_1 be bounded, continuous, and at least once differentiable.

The coupling constant λ and the pair potential V must be chosen in a manner consistent with preservation of all single-occupancy Φ_0-minimum configurations as Φ relative minima; and no new minima should be created. This will be achieved if (a) the gradient of V vanishes for nearest-neighbor adsorption sites $\mathbf{R}_i,\mathbf{R}_j$ but at no other cell-interior locations, (b) all D principal curvatures of U are positive at the adsorption site, (c) $|\lambda|$ is sufficiently small. Section III exhibits a specific way to satisfy these requirements.

Without loss of generality we can suppose that the nearest-neighbor potential for particles undisplaced from the adsorption sites is unity:

$$V(\mathbf{R}_i,\mathbf{R}_j) = 1 \,. \tag{2.8}$$

Consequently, the depths of the Φ minima are all described by

$$\Phi_\alpha = -NU_0 + N_{11}\lambda \,, \tag{2.9}$$

where N_{11} stands for the number of nearest-neighbor pairs of singly occupied adsorption sites. This is exactly the form of the energy expression which appears in the conventional discrete nearest-neighbor lattice gas models, and these in turn are equivalent to nearest-neighbor Ising models in suitable homogeneous external fields.[18] In particular, the half-filled state ($N = M/2$) corresponds to a zero-field Ising model. A knowledge of Ising model thermodynamic properties, either from exact one- and two-dimensional solutions or from a variety of approximate methods for other dimensions and nonvanishing fields, can in principle be converted to the distribution $\sigma(\phi)$ for the adsorption model.

In Sec. III we will see by concrete illustration that V can be chosen so that the steepest-descent connections between arbitrary configurations and their associated minima never force particles to leave their cells. Consequently the multidimensional basins are just direct products of ND-dimensional cells.

Let $\mu_1 \cdots \mu_M$ be a set of Ising spin variables for the unit cells of the substrate, with values -1 and $+1$ referring respectively to the empty and the occupied states. Then the depths shown in Eq. (2.9) for the various Φ minima can equally well be written:

$$\begin{aligned}\Phi_\alpha &= -\sum_{i=1}^{M}(1+\mu_i) + (\lambda/4)\sum_{\langle i,j \rangle}(1+\mu_i)(1+\mu_j) \\ &\equiv A + H_0\sum_{i=1}^{M}\mu_i + J\sum_{\langle i,j \rangle}\mu_i\mu_j \,,\end{aligned} \tag{2.10}$$

where

$$\begin{aligned}A &= [(z\lambda/8) - 1]M \,, \\ H_0 &= (z\lambda/4) - 1 \,, \\ J &= \lambda/4 \,,\end{aligned} \tag{2.11}$$

and where z denotes the lattice coordination number. In view of the fact that N is fixed in the original adsorption model, only the last term in Eq. (2.10) varies with the configuration of Ising spins.

Because we are dealing with the large-system limit, it is valid to replace the condition

$$\sum_{i=1}^{M}\mu_i = 2N - M \tag{2.12}$$

with

$$\left\langle \sum_{i=1}^{M}\mu_i \right\rangle = 2N - M \tag{2.13}$$

in the Ising model with unconstrained spins, provided that the correct external field H_1 is employed in the latter. Consequently we consider the following Ising model partition function:

$$Z(\beta,H_1) = \sum_{\{\mu_i\}} \exp\left[-\beta H_1 \sum_{i=1}^{M}\mu_i - \beta J \sum_{\langle i,j \rangle}\mu_i\mu_j \right] , \tag{2.14}$$

where J is specified in Eq. (2.11). The field H_1 differs from H_0 in Eq. (2.11), and must be chosen to satisfy Eq. (2.13) at the temperature of interest.

Starting with the Ising model partition function (2.14), standard thermodynamic manipulations provide the energy and entropy as functions of temperature. Eliminating temperature yields entropy as a function of internal energy. The connection between the adsorption model and the Ising model then gives $\sigma(\phi)$ for the former.

III. SQUARE LATTICE

The next stage requires specifying and analyzing a concrete case. This will be done in two dimensions, with a single-particle adsorption potential U displaying the translational symmetry of the square lattice. Perhaps the simplest choice for U is the following:

$$U(x,y) = \cos(2\pi x) + \cos(2\pi y) \,, \tag{3.1}$$

for which the fundamental cells are the unit squares with corners having integer coordinates. The adsorption sites have half-integer coordinates and potential depth -2, i.e.,

$$U_0 = 2 \,. \tag{3.2}$$

Figure 1 provides a contour diagram for U.

The single-occupancy condition will be enforced, of course. Within that portion of the full $2N$-dimensional configuration space obeying this restriction, the interaction potential Φ_1 will be assigned the form

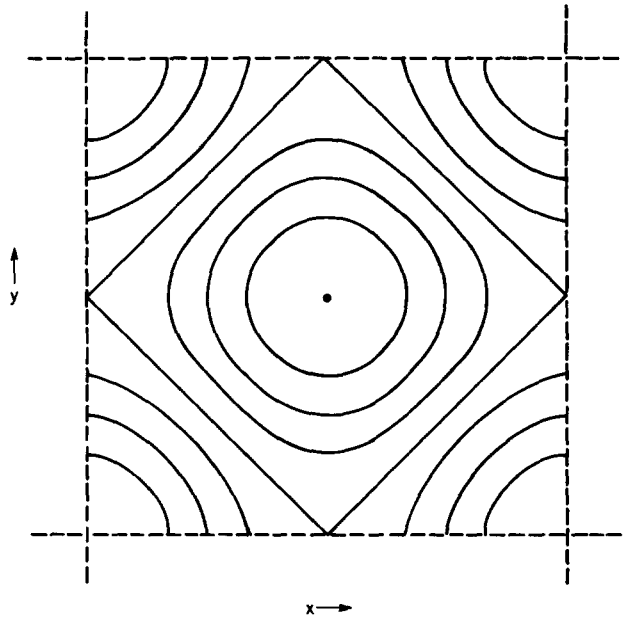

FIG. 1. Contour diagram for the square-lattice adsorption potential $U(x,y)$. Moving outward from the center of the unit cell, the contours correspond respectively to $U = -1.5, -1.0, -0.5, 0.0, 0.5, 1.0$, and 1.5.

$$\Phi_1 = \sum_{\langle i,j \rangle} \sin^2(\pi x_i) \sin^2(\pi y_i) \sin^2(\pi x_j) \sin^2(\pi y_j) , \tag{3.3}$$

where as before the $\langle i,j \rangle$ sum covers the nearest-neighbor pairs. All of the pair terms are nonnegative, and each vanishes quadratically (quartically) when either one of the two particles involved approaches an edge (corner) of the cell within which it resides. When the coupling constant λ [Eq. (2.2)] is negative, nearest-neighbor pairs are mutually stabilizing, and the corresponding Ising model is ferromagnetic. Positive λ destabilizes such pairs, and the corresponding Ising model is antiferromagnetic. In this latter case, with $N = M/2$, the absolute Φ minimum will have depth $-2N$ and will have one of the two sublattices fully occupied creating a checkerboard pattern.

By using the elementary identity

$$\sin^2 t = \tfrac{1}{2}[1 - \cos(2t)] , \tag{3.4}$$

it is straightforward to show that interparticle interactions neither destroy nor create Φ minima, compared to those already present in Φ_0, provided:

$$\lambda < 1/2 . \tag{3.5}$$

The most destabilizing situation would involve positive λ and a central particle with all four nearest-neighbor cells occupied exactly at their centers (the fiducial adsorption sites). Inequality (3.5) guarantees that even under this circumstance the central particle continues to experience a force field directing it toward the center of its cell.

The only real value of the external field H_1 for which the square Ising model has been solved exactly, is zero. Fortunately this provides an interesting case, namely the half-filled system. The corresponding results for the energy u and free energy f per Ising spin are as follows[17,19,20]:

$$u(\beta) = -J \coth(2\beta J)\left\{1 + \frac{2}{\pi}\left[2\tanh^2(2\beta J) - 1\right]K_1(\kappa)\right\} , \tag{3.6}$$

$$\beta f(\beta) = -\ln[2\cosh(2\beta J)] - \frac{1}{2\pi}\int_0^{\pi} d\theta \ln\{\tfrac{1}{2}[1 + (1-\kappa^2\sin^2\theta)^{1/2}]\} , \tag{3.7}$$

where K_1 is the complete elliptic integral of the first kind, and

$$\kappa = -\frac{2\sinh(2\beta J)}{\cosh^2(2\beta J)} . \tag{3.8}$$

The entropy per spin s follows from

$$s(\beta)/k_B = \beta[u(\beta) - f(\beta)] . \tag{3.9}$$

Remembering that there are half as many particles in the adsorption model as there are Ising spins, we can finally make the identifications:

$$\phi = -2 + 2u ,$$
$$\sigma = 2s/k_B . \tag{3.10}$$

Figure 2 indicates the behavior of the resulting function $\sigma(\phi)$. Noteworthy features include reflection symmetry across a vertical axis through the maximum that arises from invariance of the square Ising model at zero field under sign change of J. Also, the ferromagnetic and antiferromagnetic Ising models have critical points which appear as singular points in $\sigma(\phi)$, located at

$$\sigma_c \cong 0.612\,94 ,$$
$$\phi_c \cong -1 \pm 2^{-1/2}|\lambda| . \tag{3.11}$$

Owing to the logarithmically divergent heat capacity at the Ising model critical points, σ has the following behavior near its singularities (3.11):

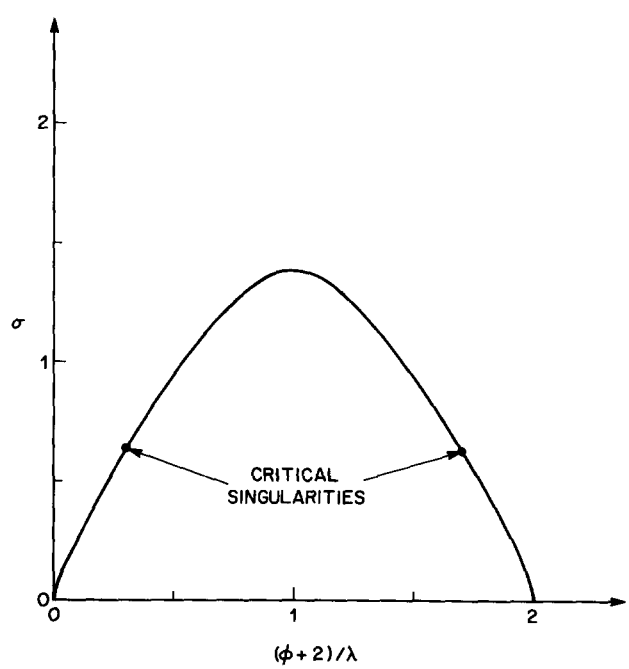

FIG. 2. The function $\sigma(\phi)$ for the square-planar adsorption model, inferred from the exact solution to the two-dimensional field-free Ising model.

$$\sigma(\phi) = \sigma_c + A(\phi - \phi_c) + \frac{B(\phi - \phi_c)^2}{\ln|\phi - \phi_c|} + \cdots , \tag{3.12}$$

where $B > 0$. Notice also that σ is singular at its endpoints, where σ' diverges.

Consistent with remarks in Sec. II, steepest-descent basins for the square lattice model are all unit $2N$-dimensional hypercubes. They contain saddle points (transition states) on their boundaries with associated reaction paths that correspond to allowed transitions of single particles between neighboring cells on the substrate. The number of such saddle points for any basin is exactly $4N - 2N_{11}$.

IV. VIBRATIONAL EFFECTS

The vibrational partition function within any hypercubical basin B_α for the square lattice model defined in Sec. III has the following form:

$$Y_\alpha(\beta) = \int_{B_\alpha} d\mathbf{r} \exp\{-\beta[2N - \lambda N_{11} + \Phi_0(\mathbf{r}) + \lambda\Phi_1(\mathbf{r})]\} , \tag{4.1}$$

where Φ_0 and Φ_1 are specified by Eqs. (2.3), (3.1), and (3.3). The basin depths for fixed N depend only on N_{11}, the number of occupied nearest-neighbor cells [see Eq. (2.9)]. Consequently the vibrational free energy f_v introduced in Eq. (1.5) can be obtained from the average of all Y_α with fixed $N_{11} \equiv N(\phi + 2)/\lambda$:

$$\exp[-\beta N f_v(\beta,\phi)] = \langle Y_\alpha(\beta)\rangle_{N_{11}} . \tag{4.2}$$

For any given basin of interest, the arrangement of the N particles in the unit cells of U will define a set of connected clusters $\{C_{i\alpha}\}$. Each connected cluster contains all particle pairs which either interact directly as nearest neighbors, or are indirectly connected through an intervening chain of nearest neighbors. It is clear that Y_α factors into contributions from separate connected clusters:

$$Y_\alpha(\beta) = \prod_i y(C_{i\alpha},\beta) . \tag{4.3}$$

If connected cluster $C_{i\alpha}$ contains n atoms, we can write

$$y(C_{i\alpha},\beta) = \int d\mathbf{r}_1 \cdots \int d\mathbf{r}_n \exp\left\{-\beta\left[2n - \lambda n_{11} + \sum_{j=1}^{n} U(\mathbf{r}_j) + \lambda \sum_{(C_{i\alpha})} V(\mathbf{r}_j,\mathbf{r}_k)\right]\right\} . \tag{4.4}$$

The individual particle integrations are restricted to unit cells specified by $C_{i\alpha}$. The specific pair interaction V for nearest neighbors in the square lattice model appears in Eq. (3.3), and one such term occurs for each of the n_{11} links in the connected cluster.

From the vibrational point of view the simplest case has $N_{11} = 0$, i.e., all pairs of particles are noninteracting. This can occur provided the system is no more than half filled. The only connected clusters then are single particles, and for those the corresponding configurational integral $y(1,\beta)$ can be carried out in closed form:

$$Y_\alpha(\beta) = [y(1,\beta)]^N \quad (N_{11} = 0) , \tag{4.5}$$

$$y(1,\beta) = \int_0^1 dx \int_0^1 dy \exp\{-\beta[2 + \cos(2\pi x) + \cos(2\pi y)]\} = \{\exp(-\beta) I_0(\beta)\}^2 , \tag{4.6}$$

where I_0 is the modified Bessel function.[21] In this simple case we have $\phi = -2$, so the corresponding vibrational free energy is the following:

$$\beta f_v(\beta, -2) = 2\beta - 2\ln I_0(\beta) . \tag{4.7}$$

From the known properties of the function I_0 we can obtain the low temperature limit:

$$\beta f_v(\beta, -2) \sim \ln(2\pi\beta) + O(\beta^{-1}) , \tag{4.8}$$

which involves only small-amplitude harmonic motion in the vicinity of the cell center. In the opposite high temperature limit, the entire square cell is accessible with equal probability, and

$$\beta f_v(\beta, -2) = 2\beta + O(\beta^2) . \tag{4.9}$$

When $N_{11} > 0$ there must be at least one connected cluster containing two or more particles. The corresponding $y(C,\beta)$ integrals are not elementary, but several of their properties can be inferred. In the high temperature limit,

$$y(C,\beta) = 1 - \beta(2n - 15\lambda n_{11}/16) + O(\beta^2) , \tag{4.10}$$

which implies a corresponding result for f_v:

$$\beta f_v(\beta,\phi) = (\beta/16)(2 - 15\phi) + O(\beta^2) . \tag{4.11}$$

In the low temperature limit small amplitude harmonic motions again obtain, and in this regime the n particles of a connected cluster C experience the following quadratic potential (measured from the potential minimum):

$$\pi^2 \sum_{j=1}^{n} [2 - \lambda z_j(C)][(\Delta x_j)^2 + (\Delta y_j)^2] , \tag{4.12}$$

where z_j is the number of nearest neighbors to particle j in the cluster. The simple form of expression (4.12) leads immediately to

$$y(C,\beta) \sim \prod_{j=1}^{n} [\beta\pi(2 - \lambda z_j)]^{-1} . \tag{4.13}$$

By assembling results (4.2), (4.3), and (4.12) we obtain the general form for the low-temperature (harmonic) vibrational free energy:

$$\beta f_v(\beta,\phi) \sim \ln(2\pi\beta) - N^{-1} \ln\left\langle \prod_{j=1}^{N} (1 - \lambda z_j/2)^{-1} \right\rangle_{N_{11}} ,$$
$$\phi = -2 + \lambda N_{11}/N . \tag{4.14}$$

The last term on the right in this expression is temperature independent, has a sign opposite to that of λ, and clearly shows the effect of particle pair interactions.

The average at fixed N_{11} in Eq. (4.14) includes all qualifying particle assignments to cells on an equal *a priori* basis. It is not valid to reorder the logarithm, averaging, and product operations in this last term to effect "convenient" simplifications. The collection of particles coordination numbers z_j appearing in Eq. (4.14) is constrained by the obvious identity

$$\sum_{j=1}^{N} z_j = 2N_{11} . \tag{4.15}$$

However, the numbers of occurrences of each of the possible

z_j values (0,1,2,3,4) can vary from one system configuration to the next. The individual products contributing to the average in Eq. (4.14) likewise fluctuate. One should keep in mind that the average (and hence its logarithm) will be dominated by products with a distribution of z_j's differing from the set of individual mean occurrence frequencies for these quantities.

When $\lambda > 0$, the antiferromagnetic case, both the high and low temperature limiting f_v expressions, Eqs. (4.11) and (4.14), show that the effect of interacting neighbors is to lower the vibrational free energy. This is easy to understand, since pair interactions reduce restoring forces toward cell centers that particles experience. The opposite occurs for $\lambda < 0$, the ferromagnetic case, where restoring forces are enhanced and f_v is increased.

Recalling the equilibrium criterion embodied in the variational Eq. (1.7), it is clear that ϕ variation of f_v (at fixed β) can have an important influence on thermodynamic properties. The logarithmic heat capacity divergence of the field-free square Ising model stems from the logarithmically vanishing curvature at ϕ_c of the $\sigma(\phi)$ function shown earlier in Eq. (3.12); sufficiently strong curvature of the f_v function with respect to ϕ could modify the nature of the heat capacity divergence at the critical point.

V. DISCUSSION

Since the models under consideration have an underlying Hamiltonian, Eq. (2.1), the particles have a well-defined Newtonian dynamics. Consequently it is possible, in principle, to study time-dependent relaxation processes and steady-state transport phenomena occurring in these dynamical lattice gases. The simple nature of the potential energy basins and of the transition states (saddle points) which connect them should be advantageous in attaining an understanding of those irreversible phenomena. It should be stressed that the present class of dynamical lattice gases differs substantially from the various "kinetic Ising models" that have been proposed,[22–24] but which involve only stochastic particle transitions between discrete locations.

Molecular dynamics computer simulation should be easily applicable to the dynamical lattice gases. In some previous molecular dynamics studies it has been illuminating, but computationally strenuous, to produce a running map of the dynamical configuration onto the relevant potential minima (by steepest-descent quenching on the potential energy hypersurface).[4,5,10,25] By contrast, this mapping is trivial for the dynamical lattice gases: simply place all particles at the centers of the cells in which they momentarily reside. One could use exact Ising model results (as explained in Sec. III) to provide checks on attainment of equilibrium and on finite-system-size effects in the molecular dynamics simulations.

Supercooling, glass transitions, and low-temperature amorphous solids are important related topics which might benefit from dynamical lattice gas studies. In particular, attention should be focused on the case of the quarter-filled ($N = M/4$) face-centered cubic lattice gas with an appropriate three-dimensional "substrate" potential and with repulsive nearest-neighbor interactions. The lowest-potential-energy state for this case has one of the four simple-cubic sublattices fully occupied, the other three vacant, to produce a long-range-ordered "crystal." At high temperature the four sublattices exhibit equal average occupancies, and the resulting "liquid" possesses only short range order. Under strict equilibrium conditions these two phases interconvert through a first-order melting or freezing transition. However, if the liquid were cooled rapidly, nucleation could be avoided and a low temperature amorphous phase would result. It would be valuable to establish how the structure of this amorphous material depends upon the details of the cooling schedule employed.[26]

Real glass-forming substances typically contain several components, or may consist of molecules with asymmetrical and variable shapes. Our dynamical lattice gases can be extended in both these directions. With several distinct components, the corresponding Ising model has spin greater than one-half. Asymmetrical molecules can also be translated into higher-spin Ising models. Polyatomic molecules that can occupy several contiguous sites however, would require an appropriate choice of nonadditive interactions in the Ising model version.

Finally, we mention that dynamical lattice gases would offer a convenient testing ground for the extended Lindemann criterion mentioned earlier.[9]

For all of these reasons, further analytical and numerical examination of dynamical lattice gas models seems amply motivated.

[1] T. L. Hill, *Statistical Mechanics* (McGraw–Hill, New York, 1956).
[2] F. H. Stillinger and T. A. Weber, Kinam A **3**, 159 (1981).
[3] F. H. Stillinger and T. A. Weber, Phys. Rev. A **25**, 978 (1982).
[4] F. H. Stillinger and T. A. Weber, Phys. Rev. A **28**, 2408 (1983).
[5] F. H. Stillinger and T. A. Weber, Science **225**, 983 (1984).
[6] F. H. Stillinger and T. A. Weber, J. Chem. Phys. **80**, 4434 (1984).
[7] T. A. Weber and F. H. Stillinger, J. Chem. Phys. **81**, 5089 (1984).
[8] F. H. Stillinger, and R. A. LaViolette, J. Chem. Phys. **83**, 6413 (1985).
[9] R. A. LaViolette and F. H. Stillinger, J. Chem. Phys. **83**, 4079 (1985).
[10] T. A. Weber and F. H. Stillinger, Phys. Rev. B **32**, 5402 (1985).
[11] F. H. Stillinger, T. A. Weber, and R. A. LaViolette, J. Chem. Phys. **85**, 6460 (1986).
[12] F. H. Stillinger, Physica A **140**, 142 (1986).
[13] F. H. Stillinger and T. A. Weber, J. Phys. Chem. **91**, 4899 (1987).
[14] T. A. Weber and F. H. Stillinger, J. Chem. Phys. **87**, 3252 (1987).
[15] *Amorphous Solids*, edited by W. A. Phillips (Springer, New York, 1980).
[16] *Glassy Metals II*, edited by H. Beck and H. -J. Güntherodt (Springer, New York, 1983).
[17] L. Onsager, Phys. Rev. **65**, 117 (1944).
[18] Reference 1, Chap. 7.
[19] C. Domb, Adv. Phys. **9**, 149 (1960).
[20] K. Huang, *Statistical Mechanics* (Wiley, New York, 1963), pp. 370–373.
[21] M. Abramowitz and I. A. Stegun, *Handbook of Mathematical Functions*, Natl. Bur. Stand. Appl. Math. Ser., No. 55 (U.S. GPO, Washington, D.C., 1964), pp. 374–378.
[22] R. J. Glauber, J. Math. Phys. **4**, 294 (1963).
[23] E. W. Montroll and H. Reiss, Proc. Natl. Acad. Sci. **78**, 2659 (1981).
[24] G. H. Fredrickson and H. C. Andersen, J. Chem. Phys. **83**, 5822 (1985).
[25] F. H. Stillinger and T. A. Weber, Phys. Rev. B **31**, 5262 (1985); **33**, 1451 (E) (1986).
[26] H. Reiss, Chem. Phys. **47**, 15 (1980).